Investigation of the sound transmission through a locally resonant metamaterial cylindrical shell in the ring frequency region

Cite as: J. Appl. Phys. **125**, 115105 (2019); https://doi.org/10.1063/1.5081134
Submitted: 14 November 2018 . Accepted: 07 March 2019 . Published Online: 20 March 2019

Zibo Liu, Romain Rumpler, and Leping Feng

Journal of Applied Physics ARTICLE scitation.org/journal/jap

Investigation of the sound transmission through a locally resonant metamaterial cylindrical shell in the ring frequency region

Cite as: J. Appl. Phys. **125**, 115105 (2019); doi: 10.1063/1.5081134
Submitted: 14 November 2018 · Accepted: 7 March 2019 ·
Published Online: 20 March 2019

Zibo Liu,[1,a)] Romain Rumpler,[1,2,b)] and Leping Feng[1,c)]

AFFILIATIONS

[1]The Marcus Wallenberg Laboratory for Sound and Vibration Research (MWL), Department of Aeronautical and Vehicle Engineering, KTH Royal Institute of Technology, SE-100 44 Stockholm, Sweden
[2]Centre for ECO^2 Vehicle Design, KTH Royal Institute of Technology, SE-100 44 Stockholm, Sweden

[a)]**Electronic mail:** zibo@kth.se
[b)]**Electronic mail:** rumpler@kth.se
[c)]**Electronic mail:** fengl@kth.se

ABSTRACT

Locally resonant metamaterial flat panels have proved to potentially exhibit extraordinary sound transmission loss properties when the resonance frequency of the resonators is tuned to the coincidence frequency region. Whether this technique is also effective to address the ring frequency effect for curved panels is investigated in this paper. For this purpose, a cylindrical shell, as a representation of curved panels, is studied from a theoretical and numerical point of view, with a specific focus on the transmission loss behaviour around the ring frequency region when the shell is mounted with local resonators. The influence from the resonators is presented and compared with that for a flat panel. An inverse effect of the resonators is observed on the sound transmission loss between the metamaterial cylindrical shell and the metamaterial flat panel when the resonance frequency of the resonators is tuned to be below or above the ring or coincidence frequency, respectively. Rather than the extraordinary improvement observed for the metamaterial flat panel, tuning such conventional resonators to the ring frequency of curved panels generates two side dips despite a sharp improvement at the ring frequency itself. This phenomenon is explained from an effective impedance point of view developed in this paper. The approach proposed and the conclusions provided may subsequently allow for the design of suitable resonators in order to resolve the ring frequency effect for curved panels.

I. INTRODUCTION

Acoustic metamaterials have been studied extensively due to their nontrivial acoustic behaviour.[1–15] The concept of acoustic metamaterials has been adapted in order to design novel acoustic panels for sound insulation purposes.[2–7,12–15] A metamaterial acoustic panel normally consists of a host panel and resonators that may be composed of, e.g., mass-spring systems. One of the potential drawbacks of a metamaterial acoustic panel is that only a limited frequency range may benefit from the behaviour of the resonators. However, it was shown that an extraordinary sound transmission loss may be achieved if the resonance frequency of the resonators is tuned to the coincidence frequency region of the host panel, by successfully overcoming the coincidence effect.[3,6,7,12,15] Consequently, it may also be worthy to consider whether this approach may be effective in order to overcome the ring frequency effect of curved panels.

Curved panels are commonly used in modern aerospace and aeronautical industries. The sound insulation properties of these structures are of great importance due to increasing environmental requirements for passenger comfort and health. In particular, the problematic ring frequency effect, associated with the curved nature of these structures, may lead to a severe deterioration on the sound transmission loss and thus demands careful considerations. Hence, there is a great need for resolving the ring frequency effect and thus improving the sound insulation properties of curved panels.

Several research contributions have been conducted to study the acoustic behaviour of curved panels of different kinds.[16–28] However, effective solutions for improving the sound transmission loss of these panels, especially over the ring frequency region, are relatively rare, e.g., compared with the attention given to the coincidence effect. Estève and Johnson[22] adopted distributed vibration absorbers and Helmholtz resonators in order to obtain a reduction of sound transmission through a cylindrical shell by tuning the resonance frequency to suppress the structural and acoustic modes. Liu *et al.*[24] employed stringers for a curved panel, which leads to a slight improvement of sound transmission loss around the ring frequency, at the expense of decreasing it above the ring frequency. In particular, to the authors' knowledge, few contributions have been made with respect to sound transmission loss properties of curved panels mounted with resonators. This may well be due to the difficulty to design effective solutions for this configuration. Indeed, unlike for the coincidence frequency, it is relatively ineffective to tune such resonators in order to overcome the ring frequency effect. This point is illustrated in a preliminary evaluation in Fig. 1, based on an impedance approach such as the one developed in this contribution. As shown in Fig. 1(b), the use of resonators in combination with curved panels in order to overcome the ring frequency effect gives rise to two side dips, considered here to be "side effects." In fact, a similar phenomenon may also be seen in a recent experimental study on the use of resonators to solve the ring frequency effect.[28] This paper is mainly focused on providing explanations for these phenomena. The physical insights drawn from the analysis may provide valuable theories for the design of suitable resonators in order to resolve the ring frequency effect of curved panels.

In order to carry out the investigation, a cylindrical shell is taken as a representation of curved panels in order to study the sound transmission loss behaviour around the ring frequency region. The influence of the resonators is systematically evaluated by varying their resonance frequency to different frequency regions, i.e., below, at, or above the ring frequency of the cylindrical shell. Both the theoretical estimation and the numerical simulations are conducted for the cylindrical shell. The theoretical derivation is based on an impedance approach developed for the infinite cylindrical shell. The numerical simulations are based on finite element models, constructed for a section of the cylindrical shell, assumed infinitely long in one direction and clamped in the other, which is a realistic representation of practical engineering situations. In order to support the explanations associated with the sound transmission loss behaviour of the metamaterial cylindrical shell, a flat panel, whose coincidence frequency is on purpose set to be about the same as the ring frequency of the cylindrical shell, is also presented. This latter test case serves as a reference in order to highlight the effect of the resonators when associated with the cylindrical shell.

The paper is organized as follows: Sec. II introduces an effective impedance approach for the sound transmission loss estimation of the metamaterial flat panel and the cylindrical shell; Sec. III presents the finite element simulations for a section of the metamaterial cylindrical shell; in Sec. IV, comparisons of the investigated panels and the explanations of the phenomena are provided; conclusions are then drawn in Sec. V.

II. IMPEDANCE APPROACH

The impedance approach is developed in order to estimate the airborne sound transmission loss of locally resonant metamaterial acoustic panels. This approach is developed in the low frequency

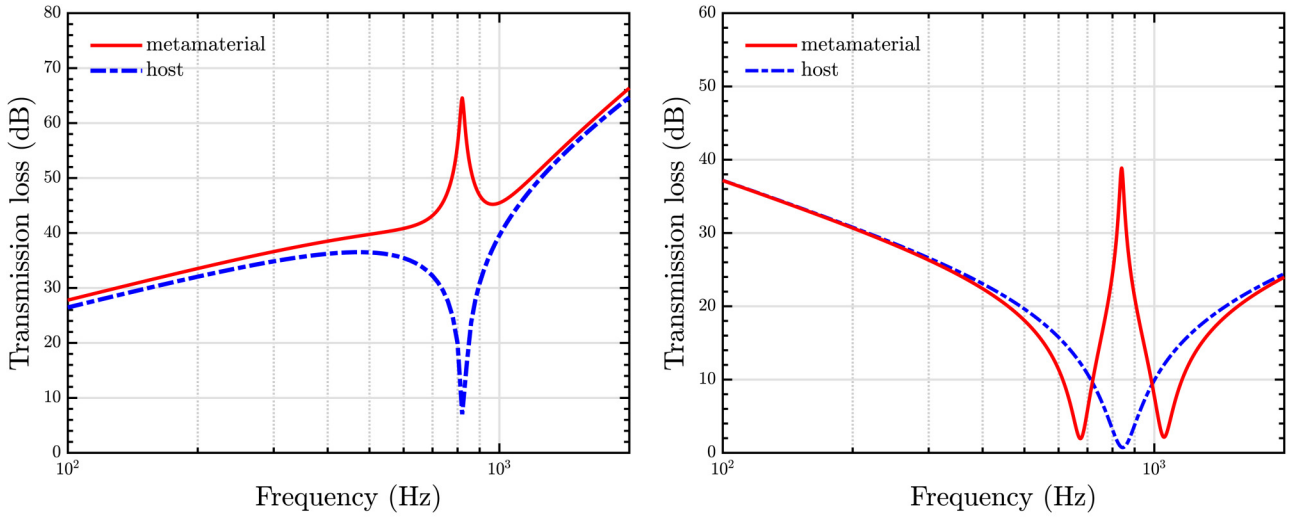

(a) Coincidence effect. (b) Ring frequency effect

FIG. 1. Illustration of the impact of tuning a conventional mass-spring resonator to the coincidence frequency (left) or the ring frequency (right).

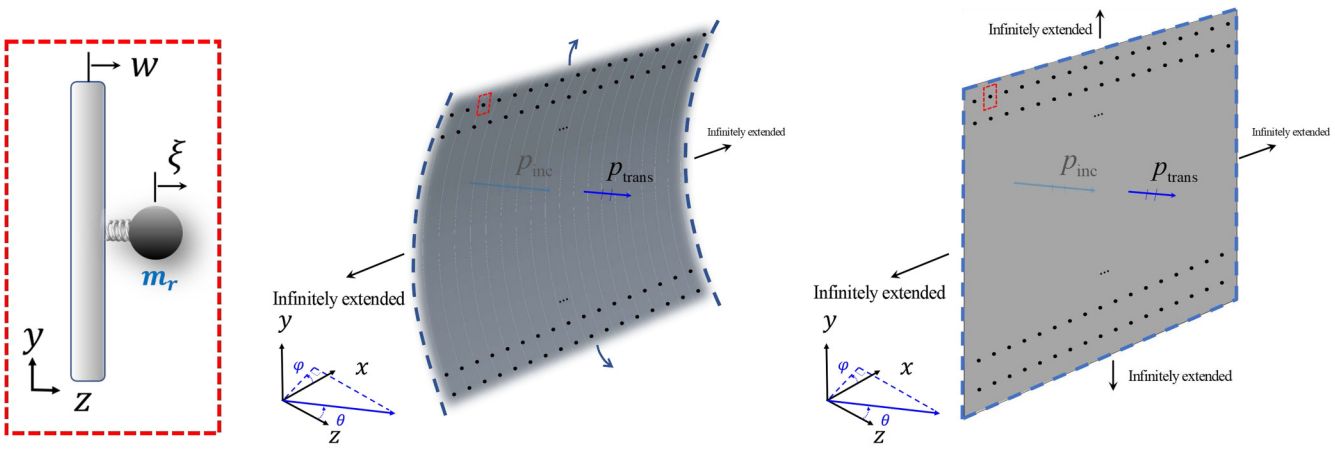

(a) Resonator. (b) Cylindrical shell. (c) Flat panel.

FIG. 2. Presentation of the locally resonant metamaterial acoustic panels studied.

range where both the thickness of the panels and the distance between resonators are much smaller than the acoustic wavelength. On this basis, the sound transmission loss of a metamaterial acoustic panel is studied by taking into account the classic airborne sound transmission model, as shown in Fig. 2. The panel is located between two semi-infinite domains and is excited by time-harmonic incident plane waves, inducing both reflected and transmitted acoustic waves. The incident angle with respect to the normal direction of the panel is θ. The azimuth angle φ, as shown in the figure, is set to be 0. The impedance of the panels may thus be derived by considering the ratio of the acoustic pressure difference to the normal particle velocity of the panel.

In order to extend the case to the metamaterial acoustic panels, an effective impedance approach is introduced. The effective impedance of a metamaterial panel may be obtained by combining the impedance of the host panel with the equivalent impedance of the resonators. By using such an approach, the sound transmission loss of the metamaterial flat panel and the metamaterial cylindrical shell may be estimated.

A. Impedance of the host panels

The impedance of an unbounded flat panel under a thin plate assumption is given by[29]

$$Z = j\omega m\left(1 - \frac{f^2}{{f_{cr}}^2}\sin^4\theta\right), \tag{1}$$

where $j = \sqrt{-1}$, m is the surface density of the panel, $f_{cr} = c_0^2\sqrt{m/D}/(2\pi)$ is the critical frequency of the panel, in which $D = E(1 + j\eta_{st})t^3/[12(1 - \upsilon^2)]$ is the bending stiffness, with E being Young's modulus, υ Poisson's ratio, t the thickness of the panel, and η_{st} the structural loss factor.

Koval[17,18] developed a simplified theory for an "infinite" slightly curved shell in order to qualitatively describe the impedance of the shell, as

$$Z = j\omega m\left(1 - \frac{f^2}{{f_{cr}}^2}\sin^4\theta - \frac{{f_{ring}}^2}{f^2}\right), \tag{2}$$

in which $f_{ring} = \sqrt{Et/m(1 - \upsilon^2)}/(2\pi R)$ is the ring frequency with R being the radius of curvature of the shell. This impedance is denoted, in this paper, as the "simplified" impedance in order to distinguish it from the more complex impedance model developed for a full cylinder mounted with resonators, which is introduced in the Appendix. In the present contribution, although this refined model has been tested and would be applicable with the methodology proposed here for fully cylindrical structures, it is only briefly mentioned in the Appendix as a natural extension.

B. Equivalent impedance of the locally resonant system

In order to evaluate the influence of the locally resonant systems on the host panel, an equivalent impedance model is developed.

Based on the notations in Fig. 2(a), the equation of motion for the resonator m_r is, similarly to the locally resonant system in one lattice of the periodic metamaterial,

$$-k(\xi - w) = m_r\ddot{\xi}, \tag{3}$$

where k is the spring constant and ξ and w are the displacement of the resonator and of the host panel, respectively. m_r is the surface density of the resonator, that is, the ratio of the mass of the resonator to the surface area of one lattice.

Assuming a time harmonic motion of the form $\xi = \hat{\xi}e^{j\omega t}$ in Eq. (3), we have

$$\frac{\hat{\xi}}{\hat{w}} = \frac{k}{k - \omega^2 m_r}. \tag{4}$$

The force of the host panel on the resonator is $\hat{F} = k\left(\hat{w} - \hat{\xi}\right)$. The equivalent impedance is then estimated by the ratio of the reaction force to the local velocity as

$$Z_{eq}^{r} = \frac{\hat{F}}{j\omega\hat{w}} = j\omega m_r \frac{1}{1 - f^2/f_{res}^2}, \tag{5}$$

where $f_{res} = \sqrt{k(1 + j\eta_{sp})/m_r}/(2\pi)$ is the resonance frequency of the resonator, with η_{sp} being the loss factor of the spring.

C. Effective impedance of the metamaterial panels

The effective impedance may subsequently be expressed as a combination of the impedance of the host panel and the equivalent impedance of the locally resonant system, such that

$$Z_{eff} = Z + Z_{eq}. \tag{6}$$

D. Sound transmission loss

The transmission coefficient may be expressed as

$$\tau = \left|1 + \frac{\cos\theta}{2\rho_0 c_0} Z_{(eff)}\right|^{-2}, \tag{7}$$

where ρ_0 and c_0 are the density and speed of sound in the air, respectively. The notation $Z_{(eff)}$ indicates that whether the effective impedance or the host panel impedance shall be adopted depends on the situation.

The sound transmission loss (STL) may be calculated subsequently as

$$STL = 10\log\frac{1}{\tau}. \tag{8}$$

The impedance approach developed in this section will be validated and compared against the finite element results in the following. Although the impedance approach is for the unbounded panels, it may also be used to approximate acoustic behaviour for the panels under a finite-sized situation as long as the size of the panel is much larger than the wavelength.[30]

Moreover, in addition to offering a very efficient approach for a preliminary study of the metamaterial structures before a more detailed and computationally-costly numerical modelling, the impedance approach also provides a basis for the physical explanation of the transmission behaviour observed with finite element simulations. The finite element simulations are introduced in Sec. III.

III. FINITE ELEMENT MODELLING OF THE LOCALLY RESONANT METAMATERIAL PANELS

In order to validate the impedance approach as well as to model the specific applications of interest, numerical simulations are presented here. These are based on the finite element method and are conducted in the commercial software COMSOL.[31]

The finite element models are constructed for both an infinite metamaterial flat panel and a section of the metamaterial cylindrical shell (see Fig. 3). The details and the mesh constituting the finite element model are presented in Fig. 4. The dimension of the mesh has been set in order to ensure the accuracy of the calculations for the shortest wavelength considered (i.e., the highest frequency of interest).

As for the metamaterial flat panel, in order to model sound transmission through an unbounded flat panel with periodically distributed mass-spring resonators, the model is constructed for one lattice. The resonators are modelled by soft, lightweight materials acting as springs and dense, stiff materials to represent localized masses, in a way similar to a previous contribution.[12] An aluminum panel is defined as the host panel. The unbounded dimension is modelled using a Floquet periodic boundary condition. The oblique incident sound field is modelled by a time-harmonic background pressure field with the elevation angle $\theta = \pi/3$ and the azimuth angle $\varphi = 0$. A non-reflecting boundary condition is introduced, using a plane wave radiation boundary condition in order to model the semi-infinite incident and transmitted acoustic fields. Structural-acoustic coupling conditions are enforced at the interface between the acoustic and solid domains.

Regarding the section of the shell, it may be represented by modelling one portion of the periodic structure, as shown in Fig. 4(b). The boundary condition in the finite direction is set to be

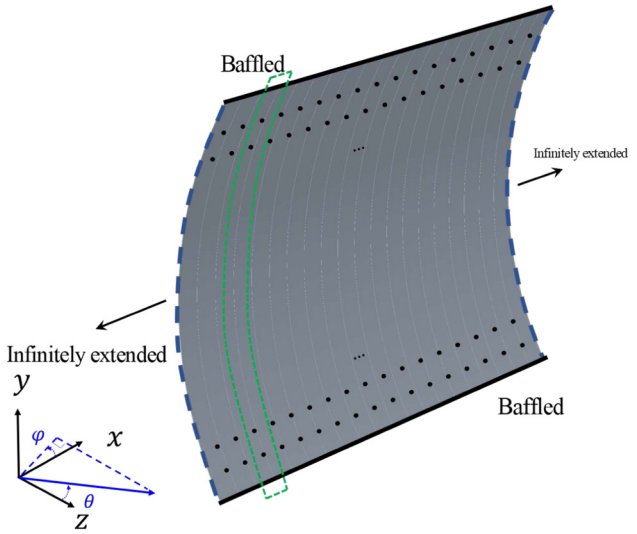

FIG. 3. Presentation of a section of the metamaterial cylindrical shell. The region enclosed by the dashed line represents a lattice of this one-dimensional periodic shell.

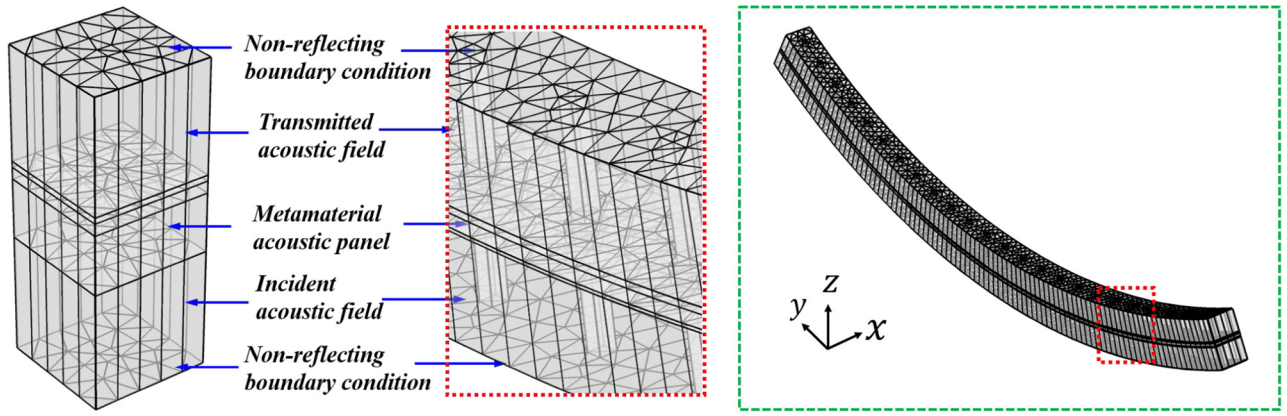

(a) One lattice of the metamaterial flat panel (left); Zoomed-in view of the lattice of the shell (right).

(b) One lattice of the section of the metamaterial cylindrical shell.

FIG. 4. Finite element models.

clamped. In the infinitely long direction, the unbounded dimension of the shell is also modelled by a Floquet periodic condition, while the non-reflecting boundary condition is modelled by a cylindrical wave radiation boundary condition in this case.

The material properties are provided in Table I. The sound transmission loss may thus be estimated from the models by

$$\mathrm{STL} = 10\log\left|\frac{\hat{W}_{\mathrm{inc}}}{\hat{W}_{\mathrm{trans}}}\right|, \tag{9}$$

where $\hat{W}_{\mathrm{inc}}$ and $\hat{W}_{\mathrm{trans}}$ are the incident and the transmitted powers, respectively.

IV. RESULTS AND DISCUSSIONS

A. Validation between the impedance approach and the finite element method

In the first step, the results based on the impedance approach and the finite element method are here validated against each other, as shown in Fig. 5.

Figure 5(a) shows a comparison associated with oblique incidence ($\theta = \pi/3,\ \varphi = 0$). The trends between the impedance approach and the finite element method are clearly the same, except for the fluctuations in the finite element results. These fluctuations are attributed to the eigenmodes inherent to the finite-sized nature of the model and the fact that only one oblique incident angle is considered in the finite element simulations.

In order to further validate the impedance approach, an averaged sound transmission loss is studied with multiple angles of incidence. The averaged sound transmission loss based on the finite element method in 1/3-octave bands is shown in Fig. 5(b). As shown, the fluctuation due to the influence of the eigenmodes is almost entirely suppressed. In fact, the more incident angles, the closer the finite element results become to the impedance approach. The reason for considering only one angle of incidence here is to extract key features with reduced computational resources. The results provided by the impedance approach thus offer both satisfying accuracy and great efficiency for the scope of the current study.

B. Sound transmission loss properties around the coincidence frequency and the ring frequency

The coincidence frequency varies according to the oblique incident angle and the thickness of the panel. For an unbounded flat panel, at frequencies below the coincidence frequency, the

TABLE I. Material properties of the host panels.

	E (Pa)	υ (–)	ρ (kg/m^3)	t (m)	Sectional angle (rad)	R (m)	f_{co} (Hz)[a]	f_{ring} (Hz)
Flat panel	6.9×10^{10}	0.3	2700	2×10^{-2}	…	$+\infty$	816	…
Cylindrical shell	6.9×10^{10}	0.3	2700	1×10^{-3}	1.85	1	1.6×10^{4}	843[b]

[a] f_{co} is the coincidence frequency of the panel. When the incident elevation angle $\theta = \pi/3$, $f_{co} = 816$ Hz.
[b] For the section of the cylindrical shell, the lowest sound transmission loss occurs at 780 Hz rather than exactly at the ring frequency; this is due to the influence of the clamped boundary condition.

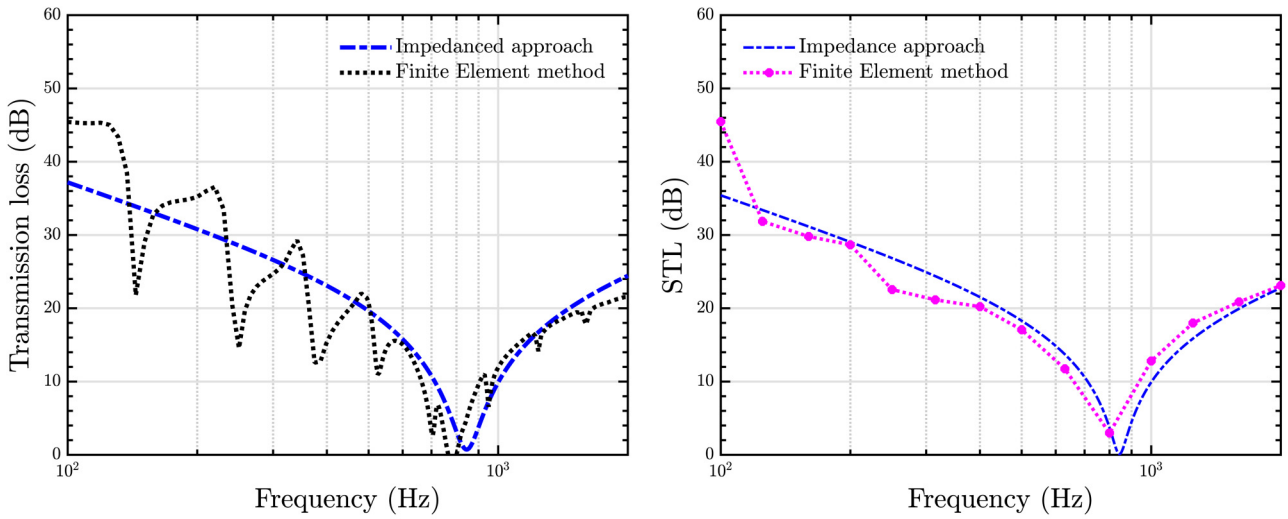

(a) One angle of incidence.

(b) Average from multiple angles of incidence.

FIG. 5. Comparison of the sound transmission loss evaluation between the impedance approach and the finite element method.

sound transmission loss is dominated by the surface density of the panel, while above the coincidence frequency, the sound transmission loss is driven by the stiffness of the panel. Accordingly, the sound transmission loss may thus be attributed to the mass-controlled region and the stiffness-controlled region, respectively.[32]

For shells with a curvature, in addition to the coincidence frequency, the ring frequency is another frequency where the sound transmission loss deteriorates, since, at such a frequency, the interaction between the bending stiffness and the membrane forces in the shell may result in a minimum impedance.[24,25] The ring frequency, in contrast to the coincidence frequency, does not change with the incident angle and the thickness of the panel. In the case of a section of a shell, the lowest transmission loss actually occurs at a slightly lower frequency than the ring frequency. A simulated displacement field at the frequency where the lowest transmission loss occurs for the section of the cylindrical shell is shown in Fig. 6. This displacement field implies that the acoustic radiation efficiency of the shell reaches a maximum value at this frequency. The influence of the curvature is shown in Fig. 7. As may be seen from

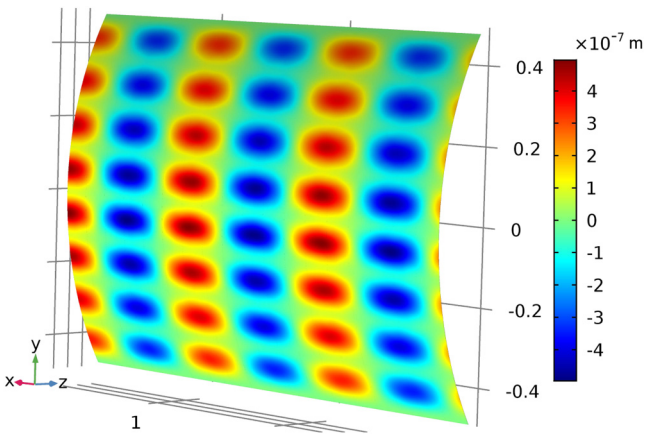

FIG. 6. Simulated displacement field in the normal direction of the surface at 780 Hz for the section of the cylindrical shell with $R = 1$ m.

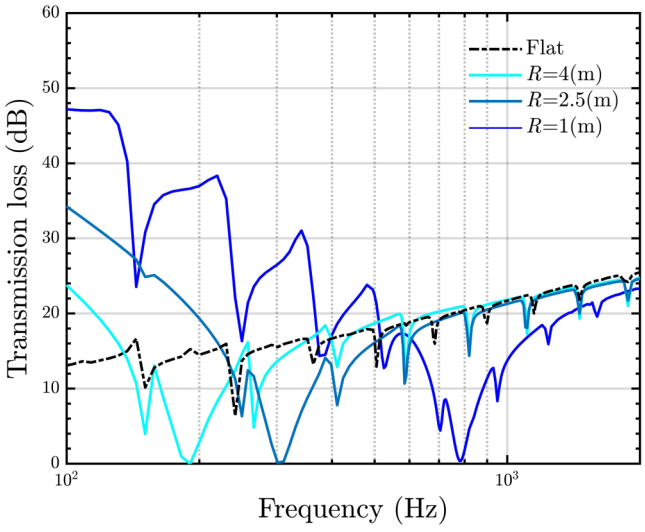

FIG. 7. Sound transmission loss of the section of the shell with different curvatures.

this plot, the ring frequency is shifted to a lower frequency as the radius of curvature increases. In addition, below the ring frequency, the sound transmission loss of a shell is better than that of a flat panel. This is due to the existence of tension forces in the curved shell, which may lead to an increased stiffness dominating the transmission loss behaviour in this frequency region. When the frequency increases to twice that of the ring frequency, the panel behaves like a flat panel, indicating that the sound transmission loss is dominated by the surface mass density of the shell in this frequency region. Therefore, contrary to the behaviour around the coincidence frequency, the sound transmission loss is stiffness-controlled below the ring frequency, while it is mass-controlled above it.

C. Influence of the resonators on the sound transmission loss

The influence of the resonators on the sound transmission loss is taken into account in this section, with a particular focus around the coincidence frequency and the ring frequency regions. Note that the incremental weight of the structure caused by the resonators in the two cases is maintained at 20% of the host panel. In order to facilitate the discussion, the coincidence frequency and the ring frequency are referred to as the specific frequencies of interest.

The influence is systematically studied by tuning the resonance frequency of the resonators to be below, at, or above the specific frequencies of interest. The results based on the impedance approach are presented, as shown in Fig. 8. When the resonance frequency is tuned below the specific frequencies of interest, a peak and a dip associated with the resonance are generated. For the flat panel, the peak appears first, followed by the dip, while these are inverted for the shell. The shift between the peak and the dip associated with the response of resonators may also be seen between the flat panel and the shell when the resonance frequency is tuned above the specific frequencies of interest.

These inverse effects of the resonators observed with the sound transmission loss are found between the mass-controlled region and the stiffness-controlled region. These opposite behaviours may be explained in terms of placing the resonance of the resonators in the mass- or stiffness-controlled regions.

As to tuning the resonance of the resonators to the specific frequencies of interest, the sound insulation behaviour of the shell, unlike for the flat panel at the coincidence frequency, results in the appearance of side dips, here denoted as "side effects," associated with the resonance of the resonators. Physically,

- for a flat panel at the coincidence frequency, the impedance is transferred from the mass-controlled region to the stiffness-controlled region,
- for a cylindrical shell at the ring frequency, the impedance is transferred from the stiffness-controlled region to the mass-controlled region.

This provides the underlying physical explanation for the ineffectiveness of tuning resonators to the ring frequency, a point that may be further explained from an impedance point of view, as detailed in Sec. IV D.

The finite element results for a section of the metamaterial cylindrical shell, as plotted in Fig. 9, also capture the behaviour of the resonators in agreement with the results of the impedance approach, thus validating the ability of the latter to estimate the overall sound transmission loss behaviour of the metamaterial panel. In particular, the resonance of the resonators in combination with the response of the host panel is well estimated by the proposed impedance approach.

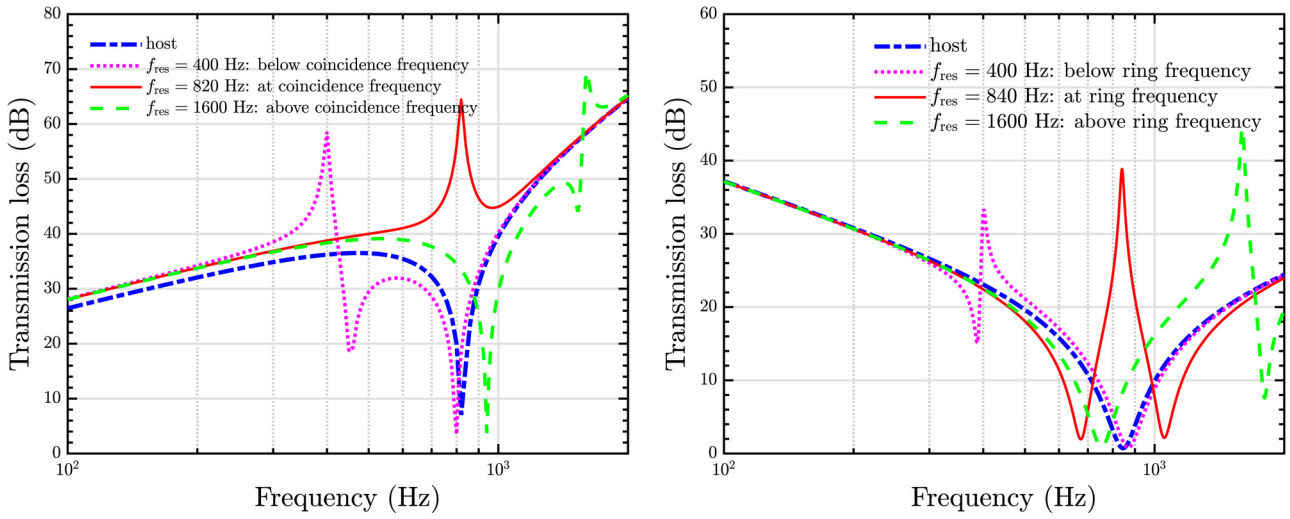

(a) Flat panel; (b) Cylindrical shell.

FIG. 8. Comparison of the influence from the resonators on the sound transmission loss between the metamaterial flat panel and the metamaterial cylindrical shell by tuning the resonance frequency of the resonators to different frequency regions.

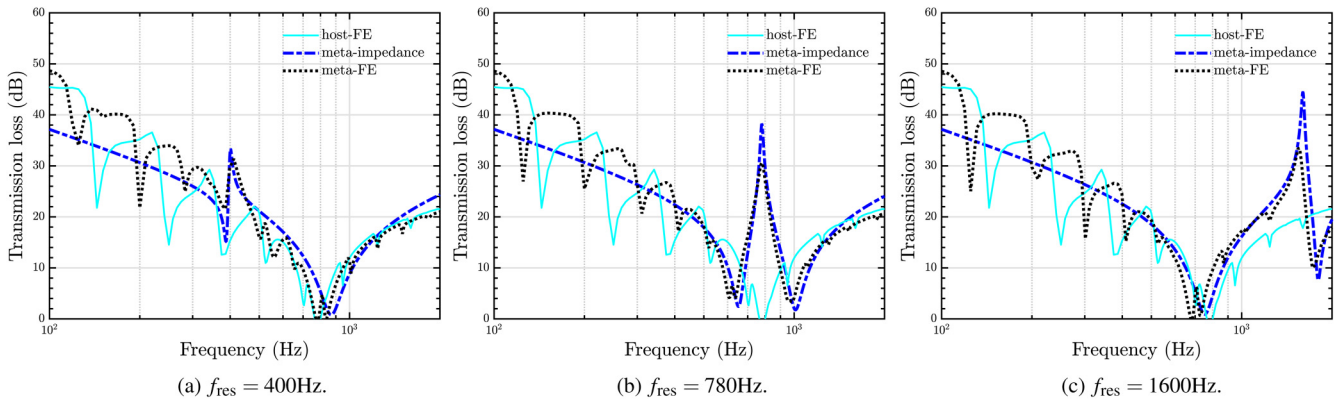

(a) $f_{res} = 400$Hz. (b) $f_{res} = 780$Hz. (c) $f_{res} = 1600$Hz.

FIG. 9. Sound transmission loss of the metamaterial shell based on the finite element modelling and the impedance approach, for the three different tuning frequencies of the resonators.

D. Analysis from an impedance point of view

In order to further detail the reasons for the extraordinary behaviour associated with the coincidence effect and the "side effects" associated with the ring frequency effect provided by the corresponding metamaterials, the impedances are studied in detail.

When the damping is small, the imaginary part of the impedance is dominant. The imaginary part of the impedance of the host panels and the equivalent impedance of the resonators are plotted in Fig. 10. As may be seen from the figure, regarding the host panel, the mass-controlled region corresponds to the region where the imaginary part of the impedance is greater than zero, whereas the stiffness-controlled region corresponds to the region where the imaginary part of the impedance is lower than zero. Regarding the equivalent impedance of the resonators, the imaginary part of the impedance changes from being positive below the resonance frequency to negative above the resonance frequency. These behaviours imply that the resonators have the same phase change as the impedance of the flat panel if tuned at the coincidence frequency, while they have an opposite phase change to the impedance of the cylindrical shell if tuned at the ring frequency.

Therefore, the cumulative effect of the impedance of the resonators and the host panels, driving the behaviour of the metamaterial panel leads to

- An increase of the absolute value of the effective impedance of the metamaterial flat panel, due to the identical phase change between the resonators and the panel (see the dashed-dotted line in Fig. 11). This results in an increased transmission loss over the entire coincidence frequency region.

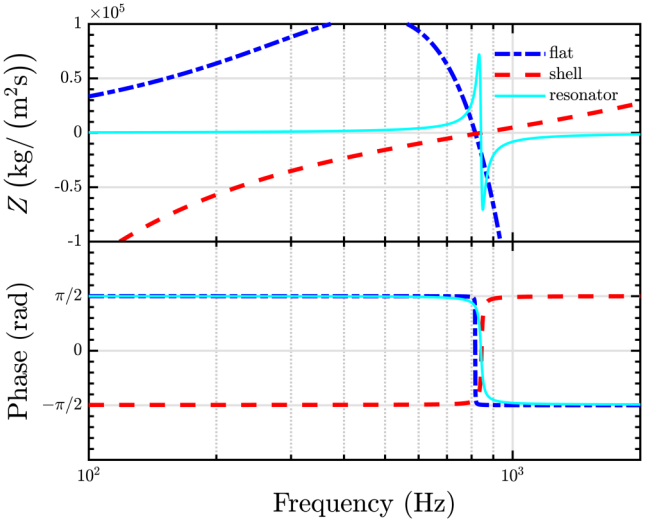

FIG. 10. Impedance of the host panels and equivalent impedance of the resonators.

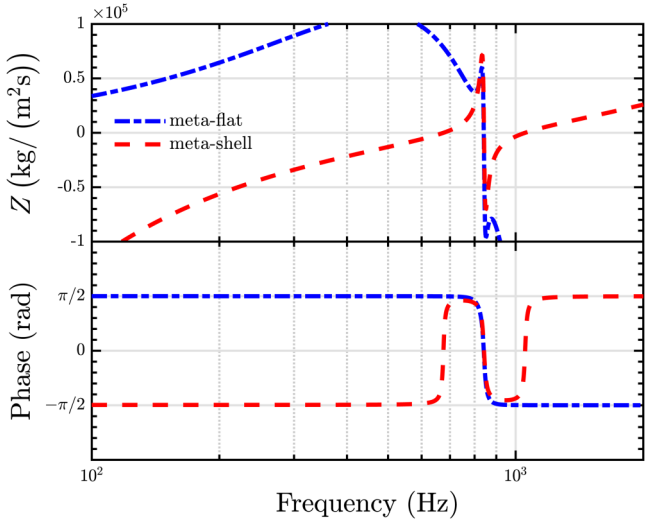

FIG. 11. Effective impedance of the metamaterial flat panel and the metamaterial cylindrical shell.

TABLE II. Sign of impedance for different subsystems and frequency regions of interest.

Z	Resonators	Flat panel	Shell
Below freq. of interest[a]	+	+	−
Above freq. of interest	−	−	+

[a]The frequencies of interest are referring to the resonance frequency, the coincidence frequency, or the ring frequency for the resonators, the flat panel, or the cylindrical shell, respectively.

- The emergence of two points where the absolute value of the effective impedance of the metamaterial shell is zero, i.e., where the impedance of the shell and the equivalent impedance of the resonators cancel each other, due to the opposite phase change between the resonators and the shell. This results in two dips at the frequencies where the effective impedance is cancelled out. Furthermore, the narrow improvement of the transmission loss in between these side frequencies is due to the resonance of the resonators (see the dashed line in Fig. 11).

The above impedance-based interpretation is further summarized in Table II, highlighting the cumulating or cancelling effects around the coincidence or ring frequencies, respectively. In practice, this implies the need to introduce resonators following the same phase change as the host panel at the specific frequencies of interest. For this purpose, the impedance approach may prove to be a powerful methodology. For the coincidence effect, this impedance approach allows one to tune conventional resonators in order to suppress the dip in the transmission loss on the basis of a systematic tuning criterion.[12] For the ring frequency, however, the impedance approach highlights that such a dip is hardly avoidable when conventional mass-spring resonators are used. In order to achieve this, specifically designed resonators may be sought, exhibiting a negative-to-positive impedance change at the resonance frequency, which cannot be achieved using conventional mass-spring resonators. The impedance approach may here open the way for the design of such unconventional resonators, e.g., considering active resonators, as one of the perspectives of this contribution.

V. CONCLUSIONS

In order to provide an explanation for the fact that conventional mass-spring resonators may not be best-suited in order to suppress the ring frequency effect associated with curved panels, a cylindrical shell was considered in this article as a representation of curved panels. It was studied using both a theoretical impedance approach and a numerical model. The comparison with the response of a locally resonant metamaterial flat panel using conventional mass-spring resonators allows one to highlight that the efficiency of such conventional resonators is governed by the change of impedance of the host panels. In the case of a flat panel with resonators tuned at the coincidence frequency, the overall effective impedance, resulting from the cumulated impedances from the resonators and the host panel, leads to an increased transmission loss without side dips. On the other hand, a similar configuration for the ring frequency of a curved panel leads to a sharp increase of the transmission loss at the expense of two side dips.

The impedance approach proposed shows that the efficiency of the metamaterial structures lies in the fact that the phase change of the impedance of the resonators should be identical to that of the host plate. As summarized in Table II, this is the case for a flat panel at the coincidence frequency, where the impedance of the host panel shifts from the mass-controlled region at lower frequencies to the stiffness-controlled region at higher frequencies. This corresponds to the behaviour of the resonator (from the sound transmission point of view), mass-driven just below its resonance frequency and stiffness-driven just above. For the curved panel, however, shifting at the ring frequency from the stiffness-controlled region at lower frequencies to the mass-controlled region at higher frequencies, the cumulative effect with the resonators leads to the cancellation of the effective impedance at two side frequencies to the ring frequency. Despite a sharp improvement at the ring frequency itself, this side effect worsens the overall transmission loss properties of the curved panel.

The proposed study further highlights the requirements for the design of suitable non-conventional resonators in order to address the ring frequency effect, based on their equivalent impedance derivation.

ACKNOWLEDGMENTS

The authors are grateful for the financial support provided by the KTH-CSC Programme (No. 201403170345). The Swedish Research Council (VR Grant No. 2015-04925) and the Centre for ECO^2 Vehicle Design (Sweden's Innovation Agency VINNOVA, Grant No. 2016-05195) are gratefully acknowledged for their financial support of the second author.

APPENDIX: IMPEDANCE APPROACH FOR A METAMATERIAL FULL CYLINDER

A more detailed description to estimate the sound transmission loss of a full cylinder mounted with resonators is further introduced based on Koval's theory,[17] with a modification derived from the effective impedance approach, as

$$\tau = \sum_N \frac{2\varepsilon_N}{k_\perp R} \Re\{Z_N^{\mathrm{c}}\} \Re\{Z_N^{\mathrm{s}}\} \left|Z_{(\mathrm{eff})\,N}\right|^{-2}, \tag{A1}$$

where

$$Z_{\mathrm{eff}\,N} = Z_N + Z_{\mathrm{eq}}. \tag{A2}$$

In Eq. (A2), Z_N is the impedance for the Nth circumferential mode under acoustic excitation of the cylindrical shell, which may be decomposed as

$$Z_N = Z_N^{\mathrm{sh}} + Z_N^{\mathrm{c}} + Z_N^{\mathrm{s}}, \tag{A3}$$

where Z_N^{sh} is the modal impedance of the shell, Z_N^{c} is the impedance associated with the interior of the cylindrical domain, and Z_N^{s} is the radiation modal impedance of the shell.

In Eq. (A3),

$$Z_N^{\mathrm{sh}} = \mathrm{j}\omega m\left(1 - A_N\frac{f_{\mathrm{ring}}{}^2}{f^2}\right),$$

$$Z_N^{\mathrm{c}} = \mathrm{j}\frac{\rho_0 c_0}{\cos\theta}\frac{H_N^{(1)}(k_\perp R)}{H_N'^{(1)}(k_\perp R)},$$

$$Z_N^{\mathrm{s}} = \frac{\rho_0 c_0}{\cos\theta}\left(\frac{2}{\pi k_\perp R}\frac{1}{J_N'^2(k_\perp R) + Y_N'^2(k_\perp R)} - \mathrm{j}\frac{J_N(k_\perp R)J_N'^2(k_\perp R) + Y_N(k_\perp R)Y_N'^2(k_\perp R)}{J_N'^2(k_\perp R) + Y_N'^2(k_\perp R)}\right), \quad \text{(A4)}$$

where

$$A_N = K\left\{\left[(k_{\mathrm{tr}}R)^2 + N^2 - 1\right]^2 + 2(1-\upsilon) \times \frac{(k_{\mathrm{tr}}R)^6 - (k_{\mathrm{tr}}R)^2N^4 + (k_{\mathrm{tr}}R)^2N^2}{\left[(k_{\mathrm{tr}}R)^2 + N^2\right]^2}\right\} + \frac{(k_{\mathrm{tr}}R)^4}{(k_{\mathrm{tr}}R)^2 + N^2}, \quad \text{(A5)}$$

with $K = t^2/[12(1-\upsilon^2)R^2]$. $H_N^{(1)}$, $H_N'^{(1)}$ are the Hankel function of the first kind and its derivation, respectively; J_N, J'_N, Y_N, Y'_N are Bessel functions of the first and second kinds and their derivations, respectively; $k_{\mathrm{tr}} = k\sin\theta$ is the trace wavenumber; $k_\perp = k\cos\theta$ is the radial wavenumber. ε_N is expressed as

$$\varepsilon_N = \begin{cases} 1, & N = 0, \\ 2, & N \geq 1. \end{cases}$$

REFERENCES

[1]J. Li and C. Chan, "Double-negative acoustic metamaterial," Phys. Rev. E **70**, 055602 (2004).
[2]Z. Yang, H. Dai, N. Chan, G. Ma, and P. Sheng, "Acoustic metamaterial panels for sound attenuation in the 50–1000 Hz regime," Appl. Phys. Lett. **96**, 041906 (2010).
[3]Y. Xiao, J. Wen, and X. Wen, "Sound transmission loss of metamaterial-based thin plates with multiple subwavelength arrays of attached resonators," J. Sound Vib. **331**, 5408–5423 (2012).
[4]M. Badreddine Assouar, M. Senesi, M. Oudich, M. Ruzzene, and Z. Hou, "Broadband plate-type acoustic metamaterial for low-frequency sound attenuation," Appl. Phys. Lett. **101**, 173505 (2012).
[5]M. Oudich, B. Djafari-Rouhani, Y. Pennec, M. B. Assouar, and B. Bonello, "Negative effective mass density of acoustic metamaterial plate decorated with low frequency resonant pillars," J. Appl. Phys. **116**, 184504 (2014).
[6]M. Oudich, X. Zhou, and M. Badreddine Assouar, "General analytical approach for sound transmission loss analysis through a thick metamaterial plate," J. Appl. Phys. **116**, 193509 (2014).
[7]H. Zhang, J. Wen, Y. Xiao, G. Wang, and X. Wen, "Sound transmission loss of metamaterial thin plates with periodic subwavelength arrays of shunted piezoelectric patches," J. Sound Vib. **343**, 104–120 (2015).
[8]Z. Hou and B. M. Assouar, "Tunable solid acoustic metamaterial with negative elastic modulus," Appl. Phys. Lett. **106**, 251901 (2015).
[9]G. Ma and P. Sheng, "Acoustic metamaterials: From local resonances to broad horizons," Sci. Adv. **2**, e1501595 (2016).
[10]S. A. Cummer, J. Christensen, and A. Alù, "Controlling sound with acoustic metamaterials," Nat. Rev. Mater. **1**, 16001 (2016).
[11]Y. Noguchi, T. Yamada, K. Izui, and S. Nishiwaki, "Optimum design of an acoustic metamaterial with negative bulk modulus in an acoustic-elastic coupled system using a level set-based topology optimization method," Int. J. Numer. Methods Eng. **113**(8), 1300–1339 (2017).
[12]Z. Liu, R. Rumpler, and L. Feng, "Broadband locally resonant metamaterial sandwich plate for improved noise insulation in the coincidence region," Compos. Struct. **200**, 165–172 (2018).
[13]Y. Liao, Y. Chen, G. Huang, and X. Zhou, "Broadband low-frequency sound isolation by lightweight adaptive metamaterials," J. Appl. Phys. **123**, 091705 (2018).
[14]J. Yang, J. S. Lee, H. R. Lee, Y. J. Kang, and Y. Y. Kim, "Slow-wave metamaterial open panels for efficient reduction of low-frequency sound transmission," Appl. Phys. Lett. **112**, 091901 (2018).
[15]T. Yamamoto, "Acoustic metamaterial plate embedded with Helmholtz resonators for extraordinary sound transmission loss," J. Appl. Phys. **123**, 215110 (2018).
[16]P. Smith, Jr., "Sound transmission through thin cylindrical shells," J. Acoust. Soc. Am. **29**, 721–729 (1957).
[17]L. R. Koval, "On sound transmission into a thin cylindrical shell under "flight conditions"," J. Sound Vib. **48**, 265–275 (1976).
[18]L. R. Koval, "Effect of air flow, panel curvature, and internal pressurization on field-incidence transmission loss," J. Acoust. Soc. Am. **59**, 1379–1385 (1976).
[19]L. R. Koval, "On sound transmission into an orthotropic shell," J. Sound Vib. **63**, 51–59 (1979).
[20]L. R. Koval, "Sound transmission into a laminated composite cylindrical shell," J. Sound Vib. **71**, 523–530 (1980).
[21]A. Blaise, C. Lesueur, M. Gotteland, and M. Barbe, "On sound transmission into an orthotropic infinite shell: Comparison with Koval's results and understanding of phenomena," J. Sound Vib. **150**, 233–243 (1991).
[22]S. J. Estéve and M. E. Johnson, "Reduction of sound transmission into a circular cylindrical shell using distributed vibration absorbers and helmholtz resonators," J. Acoust. Soc. Am. **112**, 2840–2848 (2002).
[23]S. Ghinet, N. Atalla, and H. Osman, "The transmission loss of curved laminates and sandwich composite panels," J. Acoust. Soc. Am. **118**, 774–790 (2005).
[24]B. Liu, L. Feng, and A. Nilsson, "Sound transmission through curved aircraft panels with stringer and ring frame attachments," J. Sound Vib. **300**, 949–973 (2007).
[25]B. Liu, L. Feng, and A. Nilsson, "Influence of overpressure on sound transmission through curved panels," J. Sound Vib. **302**, 760–776 (2007).
[26]F. Errico, M. Ichchou, S. De Rosa, O. Bareille, and F. Franco, "A WFE and hybrid FE/WFE technique for the forced response of stiffened cylinders," Adv. Aircraft Spacecraft Sci. **5**, 1–19 (2018).
[27]R. Talebitooti, M. Zarastvand, and H. Gohari, "Investigation of power transmission across laminated composite doubly curved shell in the presence of external flow considering shear deformation shallow shell theory," J. Vib. Control **24**, 4492–4504 (2018).
[28]C. Droz, O. Robin, M. Ichchou, and N. Atalla, "Improving sound transmission loss at ring frequency of a curved panel using tunable 3D-printed small-scale resonators," J. Acoust. Soc. Am. **145**, EL72–EL78 (2019).
[29]M. Heckl, "The tenth Sir Richard Fairey memorial lecture: Sound transmission in buildings," J. Sound Vib. **77**, 165–189 (1981).
[30]R. Lyon, "Statistical analysis of power injection and response in structures and rooms," J. Acoust. Soc. Am. **45**, 545–565 (1969).
[31]COMSOL, *Introduction to COMSOL Multiphysics* (COMSOL, 1998–2017).
[32]F. J. Fahy and P. Gardonio, *Sound and Structural Vibration: Radiation, Transmission and Response* (Elsevier, 2007).